Event Detection and its Signal Characterization in PMU Data Stream

Sanjay S. Negi, Nand Kishor, *Senior Member, IEEE,* Kjetil Uhlen, *Member, IEEE,* Richa Negi, *Member, IEEE*

***Abstract*—The potential application of signal processing techniques is not only to detect the event but also to characterize them according to physical disturbance. In this paper, event detection and its characterization algorithm is presented. The event detection scheme uses computation of spectral kurtosis (SK) on sum of intrinsic mode functions (IMF). The algorithm is capable of detecting the event in phasor measurement units (PMU) data by comparing the maximum energy and root-mean square of energy content of present analysis segment with respect to previous segment. The statistical indices applied are capable to flag specific data and thus the timely detection of events. Further, statistical features extracted from event-related segment suggest that the transient signals from different regions are distinct and thus can be classified. The signal characterization is further represented in terms of short-term energy and group delay. The analysis on event triggered signal demonstrates the related physical phenomenon in each event type. The study suggests the most relevant signal associated with a particular type of event.**

***Index Terms*—Event detection, PMU, Power grid, Monitoring, Spectral Kurtosis, Wavelet, Characterization**

I. Introduction

WIDE area monitoring is an emerging technology that can aggregate the interconnected power grid with measurements of signals via phasor measurement units (PMU) at centralized location. While a number of phasor technology applications have been already developed and as users gain experience, new applications will continue to be explored with additional tools being developed. One of the much needed applications is event characterization, which is directly related to event analysis and feature extraction [1]. The dynamic pattern of events occurrence is very well revealed by the signals available from these PMUs [2]. For example, any event due to generation/load loss in one of the region will lead to different characteristic of transient in the signal. The transient response in frequency signal will depend on individual regional grid system inertia. More specifically, the requirement of inertia to stabilize the regional grid frequency would be of different magnitude. Similarly, event involving tap-change position is more likely to bring the transient characteristic in voltage magnitude rather than frequency or voltage angle. Thus, specifying the segment/signal associated with such event would aid in adopting appropriate control action. The grid operators expect visualization techniques using advanced algorithms and intelligent tools to quickly present the received PMU data in the form of actionable intelligence [3]. The potential benefits includes reduction in cost and time in analyzing power system events and quick restorations following major grid outages. Timely event detection would provide necessary generation response and reserve requirements for a secure network [4].

During the last decade, significant research contributions on event detection have been reported. Initial work [5] described a technique using finite impulse response (FIR) filtering for detection of transients in power system following events occurrence. Use of clustering via analysing the largest initial swing of generator rotor to determine the source of an event was described in [6]. The dimensionality reduction for a large set of PMU data and event detection using Yule Walker methods [7] and principal component analysis (PCA) [8][9] were also reported in past few years. The approach was based on performance index defined in terms of prediction error calculated under normal operating conditions of the power system. An event alert was issued whenever performance index became larger than pre-specified threshold. The study [10] applied parallel detrended fluctuation analysis algorithm implemented in the MapReduce programming model and offline data mining for massive PMU data streams. The scheme computed root-mean square for every window of 50 samples long and compared with predetermined threshold to acknowledge the presence of an event. The wide area frequency signal being a common signal to respond to major power system disturbance like faults, load and generation tripping was utilized in event detection using Hodrick-Prescott Filter in [11].

But to mention here, statistical measures like minimum, maximum, mean, variance and correlation of phase angle difference though avoid computational complexity but their value depend on the length of segment, i.e. window data. This leads to difficulty in selection of threshold value for event detection. The techniques; autoregressive moving average (ARMA) and singular point based on residual modeling algorithm [12] being simple and powerful, require the inverse matrix operation for every iteration. The use of kernel direct decomposition approach for fault detection was illustrated in [13]. However, these suffer from increased computational complexity with increase in matrix size and performance

Manuscript received February 28, 201; revised May 13, 2017 and July 2, 2017; accepted July 8, 2017.
S. S. Negi is associated with Indian Railways, Allahabad, India. Nand Kishor & Richa Negi are in Department of Electrical Engineering, MNNIT Allahabad, India, Kjetil Uhlen is in Department of Power Engineering, NTNU, Norway
Corresponding author: N. Kishor (nand_research@yahoo.co.in)

deterioration in presence of noise. An improved kernel PCA combined with support vector machine (SVM) was reported in [14] for event diagnosis.

Application of advanced signal processing is an ideal tool for the task of automating the analysis of measured PMU data. Use of short-time Fourier transform (STFT) was applied for analyzing voltage signal event [15], but the performance depends on the size of window sample length. In [16], authors discussed event detection scheme using statistical measures, residual modeling, STFT and slope of phase angle signal. Wavelet analysis is established technique for non-stationary signals [17], however require appropriate sampling rate. Authors [18] have applied wavelet technique on discrete samples of collected PMU data followed by normalization based on the energy of the transformed coefficients. The energy content of decomposed wavelet coefficients was normalized against the decomposed coefficients of 1 hour PMU data samples. In [19], time-frequency representation based feature was suggested for event classification.

Little progress has been made to streamline and consolidate these detection algorithms. Many of the above techniques are not robust, reliable and thus have not sufficiently solved the event detection issue accurately on unknown types of events. For successful event analysis, it is important to realize that the final aim is not only to detect the instant at which an event occurs but also to characterize the associated event triggered signal with its corresponding physical disturbance that takes place in the power system. The underlying challenge is to extract features that relate common physical phenomenon in each event type of characteristics present in PMU signals.

This paper focuses on event detection on the continuous data stream collected via PMU installed at different locations in the power grid. The main contributions of work includes (i) events are detected without computation of any threshold, and (ii) robustness of algorithm is independent of segment length. The proposed event detection consists of two steps: 1) to detect a possible event within each data segment (or window) and 2) to locate the time-instant of significant change in magnitude. The approach applies to compare the difference of significant changes that has occurred within the data in the statistical sense on two unknown distributions, i.e. either in pre-event or post-event and event windows. The event detection algorithm is based on computation of spectral kurtosis on sum of intrinsic moment functions (IMF) and compared with those using wavelet. The event analysis is further strengthened with discussion on event associated signal property characterization, followed by classification of events based on statistical features into source of region. Further, for Nordic grid PMU data, event diagnosis step is extended to interpret physical phenomenon in each event type, i.e. to determine whether it is related to active or reactive power disturbance.

This paper is organized as follows. The signal processing techniques adopted in algorithm is described in Section II, followed by proposed event detection scheme in Section III. The description on case studies on PMU data is detailed in Section IV. In the next Section V, the results are discussed on the performance of proposed scheme and finally, the conclusions are drawn in Section VI.

II. Signal Processing Techniques

This section presents the signal processing techniques that are applied for detection of events and quantify the dynamics of signals, following the disturbances.

A. Wavelet coefficient (WC):

Using wavelet although provides variable time-frequency resolution at different frequencies, however requires proper selection of wavelet parameters through iterations increasing the computational time. The segmented signal is transformed into a sequence of coefficients at different scales. The segment $S(t)$ can be represented by coefficients $\theta_{l,k}$, scale factor l and translation factor k for basis function $\varphi_{l,k}$ given as:

$$S(t) = \sum_k \quad \sum_l \theta_{l,k}\, \varphi_{l,k}(t) \tag{1}$$

The wavelet analysis for the segment having transient event maps the coefficients of high amplitude at lower scales. While those without any transient, their decomposed coefficients are not of high amplitude at same scales. The transformed coefficients having greater concentration of energy correspond to a particular event, while those having lowest amount of energy imply to normal condition of the grid. The detail study using wavelet decomposition of PMU data for event detection can be referred from [18].

B. Empirical mode decomposition (EMD):

The EMD first introduced by Huang et al. [20] is capable to adaptively decompose any signal into a set of L_I level of complex-valued oscillating components, known as intrinsic mode functions (IMF) and a residual representing the trend. These IMF define phase information for the real and imaginary components locally. Mathematically, the set of IMF, $\{I_l(t)\}_{l=1}^{L_I}$ and a residual value is expressed as:

$$S(t) = \sum_{l=1}^{L_I} I_l(t) + r(t) \tag{2}$$

The IMF extraction from the data segment is based on an iterative method known as shifting algorithm and it can found in [21].

C. Spectral Kurtosis:

The spectral kurtosis (SK) is a spectral descriptor that overcomes the inefficiency of power spectral density for detection and characterization of transients in a signal [22]. Some applications of SK for fault detection are described in [23-25]. In simple terms, spectral kurtosis (SK) is defined as the normalised fourth-order moment of the real part of the STFT [26]. The SK is an extension of statistical measure of kurtosis defining the impulsivity of the event present in the signal in the frequency domain. The SK is computationally less expensive and fast, and reported for on-line applications in [27]. Defining the signal $Y(t)$ as the response of the system with time-varying impulse response $h(t,s)$, excited by signal $U(t)$. Thus,

$$Y(t) = \int_{-\infty}^{t} h(t-\tau)U(\tau)d\tau \tag{3}$$

For non-stationary signal, $h(t,s)$ refers to causal impulse response at time t of a system excited by an impulse at time $t-s$, then

$$Y(t) = \int_{-\infty}^{t} h(t,t-\tau)U(\tau)d\tau \tag{4}$$

In frequency domain, above equation becomes

$$Y(t) = \int_{-\infty}^{\infty} e^{j2\pi ft} H(t,f)dU(f) \tag{5}$$

Where, $H(t,f)$ is time-varying transfer function (TF) of the system, which may be assumed as the complex envelope

signal $Y(t)$ at frequency point f. Consider $H(t,f)$ conditioned at given ω, a random variable of filter's time-varying characteristic. Subsequently, the 2nd-order $(2n)$ instantaneous moment that measures the strength of the energy of the complex envelope at time t and frequency f can be given as:

$$M_{2nY}(t,f) = \frac{E\{|H(t,f)dU(f)|^{2n}\omega\}}{df} = |H(t,f)|^{2n} M_{2nU} \quad (6)$$

The defined instantaneous moment decomposes the energy contained in $Y(t)$ over the TF plane (t,f) at $n=1$.

Now, the fourth-order spectral cumulant of a non-stationary signal $U(t)$ can be given as

$$C_{4Y}(f) = M_{4Y}(f) - 2M_{2Y}^2(f)\ ,\ f \neq 0 \quad (7)$$

A larger deviation of signal from Gaussianity results into larger value of Eqn.(7). Ideally, SK assumes zero values at those frequencies corresponding to stationary Gaussian noise and high positive values at frequencies accompanied by transients due to events in the signals [26]. The SK is then defined as

$$K_Y(f) = \frac{C_{4Y}(f)}{M_{2Y}^2(f)} = \frac{M_{4Y}(f)}{M_{2Y}^2(f)} - 2\ ,\ f \neq 0 \quad (8)$$

Therefore, the energy-normalised fourth-order spectral cumulant measures the peakiness of the probability density function of the process at frequency f. The square-root of SK (SRSK) is then computed on excited signal $U(t)$, which is the processed signal, i.e. coefficients of details (CD) or sum of IMF obtained via EMD technique on the segment of PMU signals.

III. Detection And Analysis Scheme

It is expected in future, that the operators will be issued alert message through real-time detection of abnormal events that often occur in power system. On particular event detection, the next step is to extract event related characteristics and classify them so as to quickly provide actionable information for decision making. For example, the raise of alarm on the occurrence of a particular event will trigger the online estimation of state dynamics [28]. This calls analytical tools to not only detect events but also recognize their characteristics.

A. Segment Processing

Consider a large scale PMU N_P deployment in wide-spread power grid network, each providing p measurement of signals. Typically, a PMU measures $p=5$ time series bus data; frequency (F_r), active power (P), reactive power (Q), voltage angle (A_g) and voltage magnitude (V). A total of $Z = N_P \times p$ measurements are thus collected at every time instant. The architecture for event detection in PMU data, characterization and classification is depicted in Fig. 1. As illustrated in Fig.1(a), the PMU data is segmented into fixed-length window of m samples being available at a rate of 50 or 60 Hz. Each segment $S = [\vartheta_1\ \vartheta_2\ \ldots \vartheta_m]$ is a sequence of samples ϑ_i. Once the length of initial data segment equals to selected size of samples, the detection algorithm is initiated and updated after every m samples. The event detection algorithms based on computation of WC/IMFs are applied on each segment. The algorithm determines if the new data segment in analysis has characteristics different from the previous/post segment to indicate an event. In other words, an assessment is made to check if post-event (normal) dynamics has reached steady state condition. It is emphasized to discriminate between normal and event conditions. The implementation of detection algorithms; wavelet and EMD are shown in Fig. 1(b) & (c) respectively. The best mother wavelet and its level selection follow the study discussed in [18]. Using wavelet, each data segment is decomposed to L_w levels of coefficients of details (CD) from which square-root of SK (SRSK) are computed. This approach henceforth in rest of the paper is referred as SKSK-WC and suggested in Fig.1(b). Similarly, IMF of levels L_I are extracted for each segment. In the proposed scheme, SRSK is obtained for the sum of IMF upto level L_I of IMF. This computation of SRSK on sum of IMF referred as SRSK-IMF can be seen in Fig. 1(c). Both the detection schemes are applied to calculate the detection statistical indices. The computed statistical signatures on the analysis segment are compared with those obtained on previous/post segment over the complete data length. The advantage of proposed event detection scheme based on SRSK-IMF over SRSK-WC is reduced complexity in defining the algorithm parameters. This simple approach may allow development of heuristics on event signal that remove much of the conservatism. As discussed above use of wavelet analysis requires appropriate segment length, selection of mother wavelet, its coefficient level, etc.

B. Computation of Event Detection Indices

In order to detect event in the segment, detection indices; root-mean-square energy (RMSE) and maximum of energy content is calculated from the SRSK-WC and SRSK-IMF schemes. The total energy content of wavelet coefficients can be given as:

$$E_w(m;z,L_w) = \sum_{l=1}^{L_w} \sum_{k=1}^{N_c} \left|CD_{l,k}(z)\right|^2 \quad (9)$$

Then the RMSE of WC on each segment can determined from:

$$RMSE_w = \sqrt{\frac{1}{z} E_w(m,z,L_w)} \quad (10)$$

To quantify the strength of processed signal, maximum energy content can be defined as:

$$E_w^{max} = Max\{E_w(m,z,L_w)\} \quad (11)$$

Where, z is number of coefficients, N_c is number of coefficients in each decomposition level l, L_w is wavelet decomposition level.

Next, considering decomposition of segment into L_I level IMF, their total energy content can be determined from

$$E_I(m;L_I) = \sum_{l=1}^{L_I} |I_l(m)|^2 \quad (12)$$

Similarly, RMSE and maximum energy content is given as

$$RMSE_I = \sqrt{\frac{1}{z} E_I(m;L_I)}\ \&\ E_I^{max} = Max\{E_I(m;L_I)\} \quad (13)$$

These detection indices can be useful in quantifying the event associated signal characteristic. For example, if the RMSE value is high over several past segments in frequency (F_r) signal, it could be an indication that there is a significant active power unbalance. On the other hand, if a high value RMSE is detected in only one segment, this is an indication of a transient nature of event, for example a short circuit, line trip or similar event. Similarly, combined with possible signal's information about amplitude and oscillations in the test signals, the value of high RMSE can be used to indicate critically low damping of electro-mechanical modes or slow oscillations in frequency signal. For each event detected in the

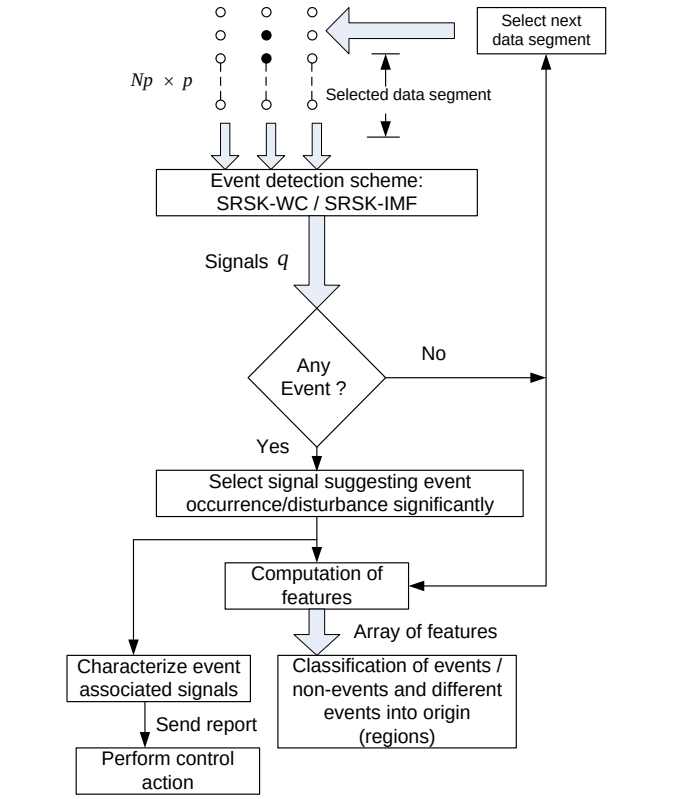

(a) Event detection and classification scheme

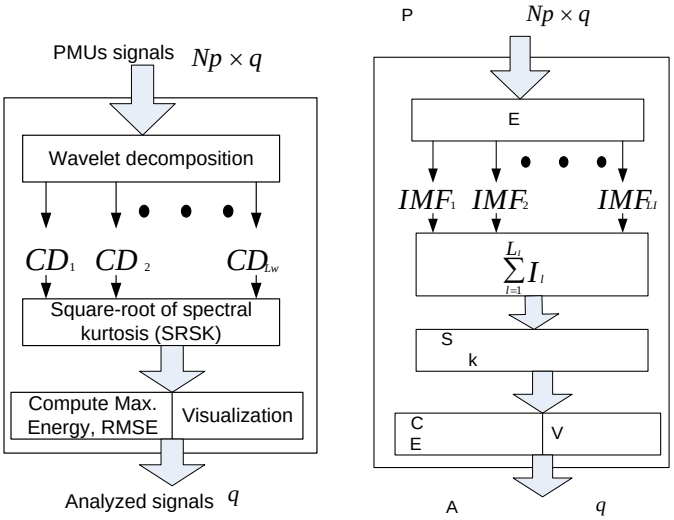

(b) Detection using SRSK-WC (c) Detection using SRSK-IMF

Figure 1. Proposed event detection, characterization and classification flowchart

different signals (F_r, P, Q, A_g or V) during the execution of algorithm, the signal that captures the strongest disturbance is subsequently characterized (Fig.1(a)).

C. Event Signal Characterization

With event signal characterization, the scheme must reflect properties of signal as much as possible. Thus, event characterization is directly related to event analysis and feature extraction. As an example, the group delay function is the negative derivative of the unwrapped short time phase spectrum. The group delay function is effective in extraction of system parameters for a minimum phase signal. In fact, the group delay is defined as the negative derivative of the Fourier transform phase. Mathematically, the delay function is defined as:

$$\tau(\omega) = -\frac{d(\phi(\omega))}{d\omega} \quad (14)$$

Where, the phase spectrum $\phi(\omega)$ of signal is defined as a continuous function of ω. The group delay function is computed from the signal, which is given as [29]:

$$\tau(\omega) = -j\frac{d(\log(X(\omega)))}{d\omega} = \frac{X_R(\omega)Y_R(\omega)+Y_I(\omega)X_I(\omega)}{|X(\omega)|^2} \quad (15)$$

Here the subscripts R and I denote the real and imaginary parts of the Fourier transform. $X(\omega)$ and $Y(\omega)$ are the Fourier transforms pairs of sum of IMF $I_l(m)$ and $mI_l(m)$ upto L_I level. The event associated signal inherently being non-stationary, its statistical properties vary across the time. Thus, another characterization property is based on calculation of distribution of energy during the event occurrence period. In other words, each analysis segment is considered of shorter duration known as a frame length with 50% overlapping. The peak of short-term energy (SE) is centered at frame length. The SE on frame length m_f is an indication of burst in the event signal defined as sum of squares of the amplitudes in a frame of sum of IMF, i.e.

$$E_I^{m_f}(m_f; L_I) = \sum_{l=1}^{L_I} |I_l(m_f)|^2 \quad (16)$$

D. Computation of Features for Events Classification

Having detected the event occurrence in a segment of the PMU signal, the next stage of diagnosis should be to classify the transient characteristic of signals. This step represents transients of similar class due to same physical disturbance from one or more regional grids, belong to one group. This ensures possibility to adopt corrective control action appropriately. Use of support vector machines (SVM) provides very good accuracy in high dimensional feature spaces. SVM as a classifier has been successfully reported for classification of islanding and different PQ disturbances [30] and the details can be referred from the references therein.

IV. PMUs Data Case Studies

A. NASPI PMU Data

The accessed NASPI PMU data (at 60 Hz) is analyzed according to the grid interconnections between the regions [31]. The angle difference signal between the regions; R1 (Central-South angle: CSA), R2 (North-South angle: NSA), R3 (West-South angle: WSA) & R4 (East-West angle EWA) clearly suggests the transients, masked by oscillations as shown in Fig. 2. Each region for e.g. R3 reflect five distinct events; A, B, C, D & E with regard to the presence of transients as suggested from Fig. 2(b). These events of one region are synchronized with the transient features of other regions. It may be seen these events are associated with significantly increased magnitude against non-event, i.e. post-event period. The analysis is performed on each data segment consisting of 1000 samples corresponding to event and post-event duration. The transient peak of region R4 is in opposite phase against those of regions R1-R3 as suggested in Fig. 2(c). Such analysis will assist to quantify the amount of control action needed in each regional grid with regard to impact of any physical disturbance leading to events in the interconnected network.

B. Nordic Grid PMU Data

Another collected time-series data considered in study is from Nordic grid network. The PMU signals; frequency and voltage magnitude are sampled at 50 Hz. The events associated with real power disturbance primarily leads to transient in frequency and voltage magnitude signals while, reactive power affects the voltage magnitude (locally) only [18]. The PMU signals accompanied with events are shown in Fig. 3. The visual inspection of signals corresponding to cases I & II indicate an occurrence of transient event.

V. Results and Discussion

This section presents the performance of above described event analysis schemes.

A. NASPI Data:

As discussed in above section, from Fig. 4(a), it is important to realize that the wavelet decomposed coefficients has highest amplitude at lower most, i.e. 4th scale. The computed SRSK from WC is shown in Fig. 4(b). The peak of SRSK remains unchanged with respect to peak of WC. Further, for non-event segment, the variation of WC at decomposed levels is not accompanied by increased magnitude. This is illustrated in Fig. 4(c). Numerically due to normalization of PMU data, as expected, the sum of wavelet coefficients is of low amplitude and fails to detect event occurrence against non-event conditions. The SRSK obtained on sum of IMF of angle signal for segment corresponding to events/post-event is shown in Fig. 5. In Fig. 5(a), the transient event A as observed is accompanied with many folds increased peak amplitude. On other hand, the variation of SRSK computed on sum of IMF for post-event segment remains in same range of amplitude as sum of IMF. Further, the variation of SRSK for remaining events as illustrated in Fig. 5(c) are also associated with significant sudden changes in amplitude. The distinct variation of event signal is thus reflected here due to same physical disturbance.

Off-course this is visual inspection and quite cumbersome in analysis for several sets of PMU signals and thus practically not feasible. It is therefore necessary to translate the signal information to take into account multiple characteristics such as time, magnitude, phase, etc. The detection indices; maximum energy and RMSE exploit the presence of event in the segment of frequency and voltage angle signals. The RMSE is a statistical measure of the magnitude of varying signal. Fig. 6 shows the bar graph of RMSE of each event/post-event computed from SRSK on WC and IMF. In Fig. 6(a), it is clear that RMSE computed from segment of angle signal having event occurrence is significantly of higher magnitude against those of post-event. As an example, adopting SRSK-WC, the RMSE ratio of event B to post-event is approximately 0.18/0.045= 4. On other hand, as indicated in Fig. 6(b), the same index when computed on IMF gives ratio of 7.0/0.5 = 14 (event B) for region R3. It can be seen that RMSE obtained on SRSK-IMF results in comparatively of higher magnitude with respect to SRSK-WC. Thus, the characteristic of event condition is preserved. This provides a wider range for event conditions against post-event, i.e. capable to magnify the difference between event and post-event. In other words, if significant amplitude of maximum energy and RMSE is identified in an adjacent segment, an event alert may be alarmed. In order to demonstrate the effectiveness of SRSK-IMF, its performance is compared with SRSK-WC and shown in Fig. 6(c). The distinction between the signals from the different regions, originating due to event occurrence is of strategic importance to adopt appropriate remedial control action schema. The comparison of index calculated for angle against frequency signal is illustrated in Fig. 6(d). In general, angle signal is subjected to increased amplitude variation with respect to frequency.

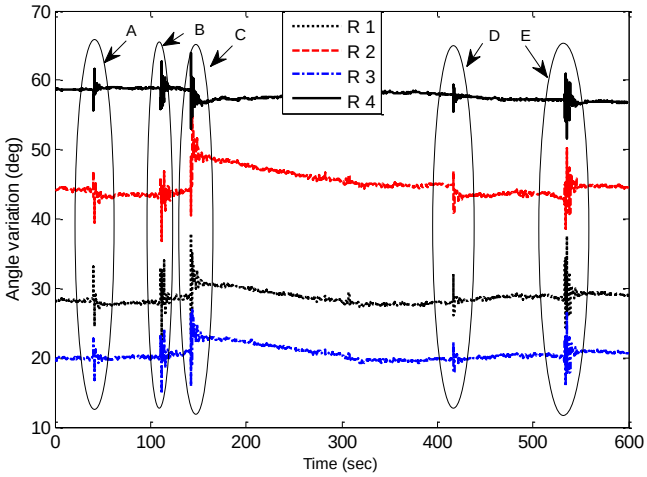

(a) Five events of four regions

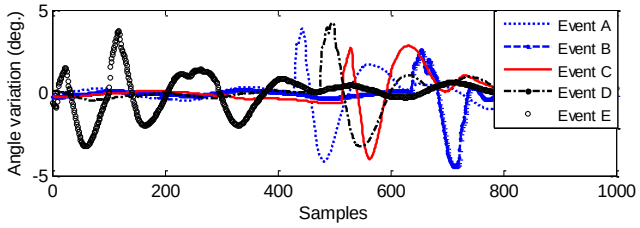

(b) Five events of region R 3

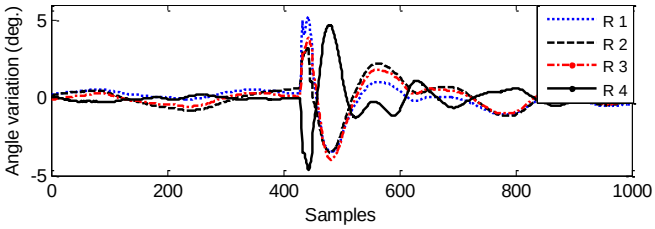

(c) Event A in four regions

Figure 2. Voltage angle variation of NASPI PMU data

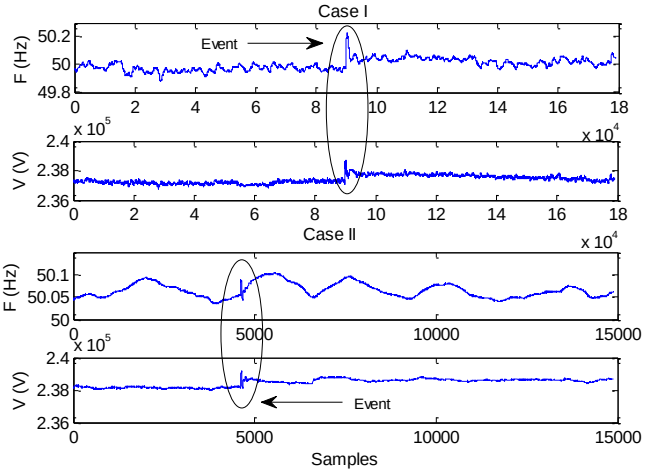

(a) Case I & II

Figure 3. Signal variation of Nordic grid PMU data

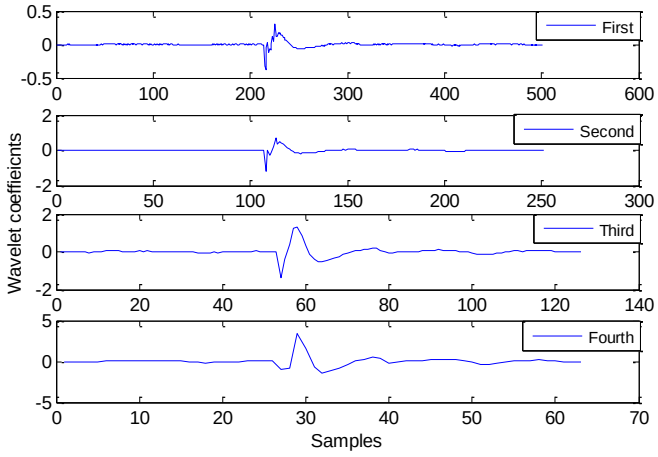

(a) Wavelet coefficients for segment with event-A

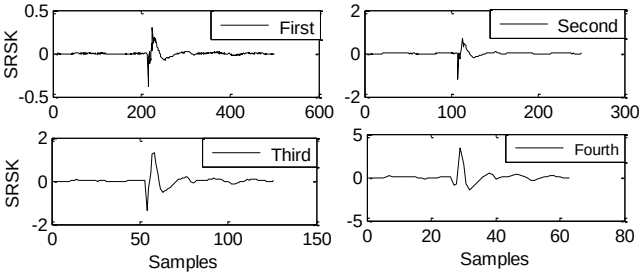

(b) SRSK computed on wavelet coefficients for segment with event-A

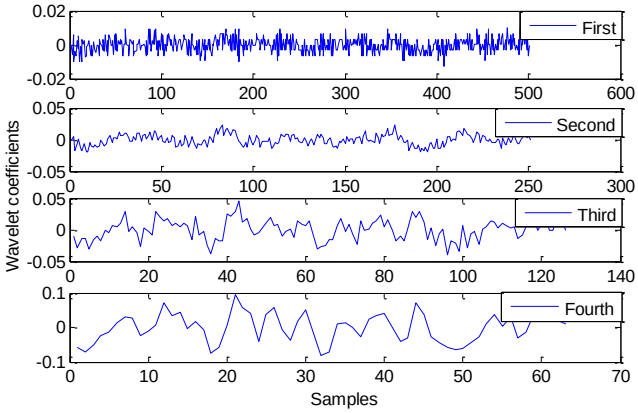

(c) Wavelet coefficients for segment with post-event- A

Figure 4. Analysis using wavelet for angle signal of region R 3

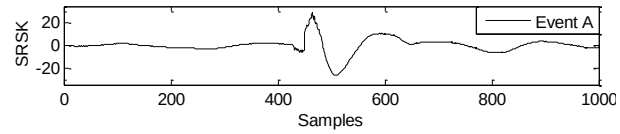

(a) SRSK computed for segment with event-A

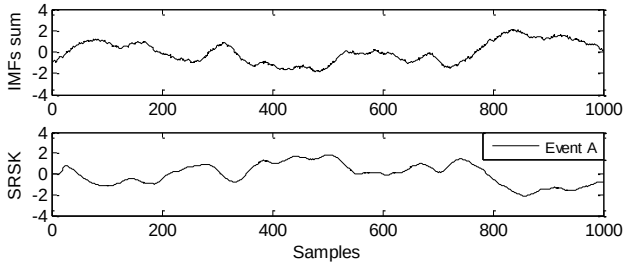

(b) SRSK computed for segment with post-event-A

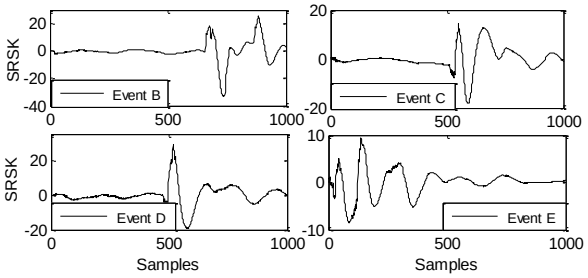

(c) SRSK computed for segment with other events

Figure 5. Analysis using EMD for angle signal of region R 3

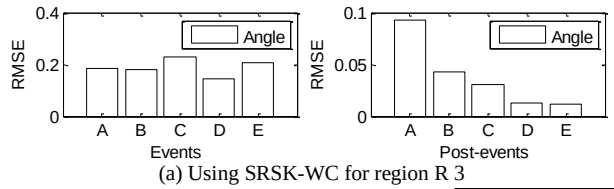

(a) Using SRSK-WC for region R 3

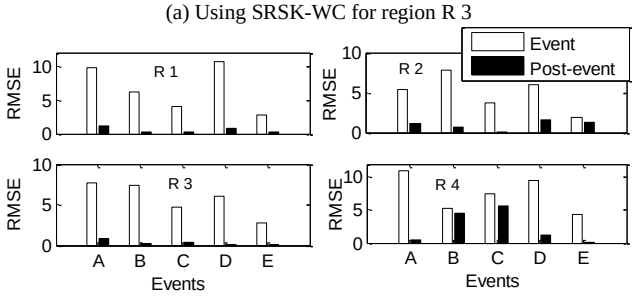

(b) Using SRSK-IMF for angle signal

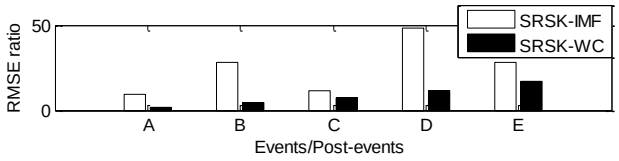

(c) Ratio of events to post-events for angle signal of region R 3

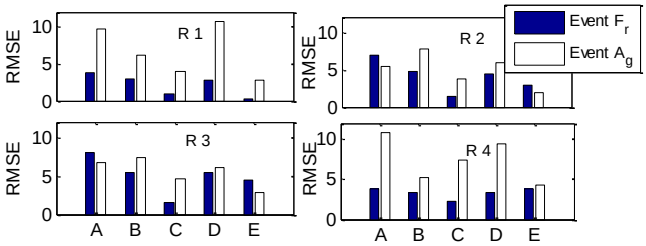

(d) Using decomposed IMF for angle and frequency signals

Figure 6. Computation of indices for signals of different regions

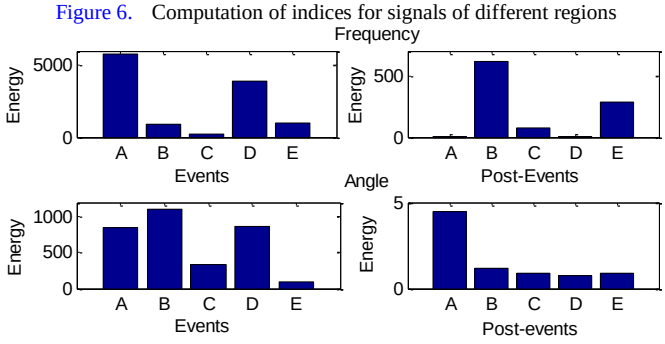

Figure 7. Maximum energy calculation using SRSK-IMF for R 3

With close observations in regions R1 & R4, it is clear that event detection using angle signal as compared to frequency signal is associated with higher magnitude of RMSE value for all the events. In other words, this also means, active power

disturbance like generation output power change leads to resultant mismatch (active power) of different magnitude in these regions and oscillations in signal (angle) die out according to its damping effect in the regions.

On other hand, in regions R2 & R3, use of frequency signal signifies comparatively better detection of events; A & E, while angle signal for events; B, C and D. This suggests comparatively large active power unbalance but good damping effect (angle signal) was achieved, causing angle oscillations to die out soon for events A & E in the grid. Similarly, computation of maximum energy for each events/non-events is illustrated in Fig. 7. It is obvious that maximum energy content is largest for segment with events against non-events and differs for every event. In respect to event detection, use of angle signal indicates a higher ratio for events with respect to non-events. It indicates that maximum magnitude of change (energy content) is observed in frequency signal following an event occurrence unlike angle signal. For e.g. event A, this interprets that physical disturbance caused largest mismatch of active power leading to maximum frequency excursions.

The distribution of SE indicated in Fig. 8(a) follows the variation as discussed above (see Fig.2(a)). For instance, SE of event E represents its burst at the beginning and decay over the frames. On other hand, the peak of remaining events is at par with their corresponding time variation. In Fig. 8(b), the SE suggests moments of high energy, being centered/spread over the frame length. The group delay estimation of event segment with respect to its own self is zero. This is clear from Fig. 8(c). For e.g. considering encircled case in said figure, the group delay of R3 is zero with respect to its own event segment. Further, group delay of R3 with respect to R4 is negative against those of regions R1 & R2. This is in accordance to phase variation in time-domain as discussed in above section.

A key aspect of a decision-making framework is not only to detect event accurately, but also to classify the characteristic of event associated signals in different regions. Thus, the proposed architecture allows to classify event/post-event signals according to their occurrence in different regions (on NASPI PMU data). In order to achieve this, once an event is detected, a feature vector is extracted from the sampled segment in time-domain. Classifier statistical features like, mean, variance, standard deviation, kurtosis and entropy [30] are calculated and used as input to the SVM classifier for classification of transient signal. The classification of event A and its post-event of R1 is depicted in Fig. 9(a). As observed, the features of signals corresponding to event A and its post-event are distinctly represented. The feature vector of data segment corresponding to all events of a particular region is classified against those of other region(s). The classifier performance is illustrated in Fig. 9(b). An accurate classification of all events occurrences in R1 against R2 as binary class is suggested. This distinct representation of event signals from each region is associated with different regional grid activity. In other words, this implies for different quantum of control action in each area depending upon the corresponding transient nature.

The classifier indices [32] are further computed to assess its performance, which are defined in terms of sensitivity, specificity and accuracy. The sensitivity, specificity and accuracy are given in form of true positive (TP), true negative (TN), false negative (FN), and false positive (FP). True positive rate (TPR) of the classifier is:

$$TPR = \frac{TP}{(TP+FN)} \quad (17)$$

False positive rate (FPR) of the classifier is:

$$FPR = \frac{FP}{(FP+TN)} \quad (18)$$

And TPR is equivalent to Sensitivity and FPR is equivalent to $(1 - \text{Specificity})$ which is turn given as:

$$\text{Sensitivity} = \text{TP}/(\text{TP} + \text{FN}) \quad (19)$$

$$\text{Specificity} = \text{TN}/(\text{TN} + \text{FP}) \quad (20)$$

$$\text{Detection accuracy (DA)} = (\text{TN} + \text{TP})/(\text{TN} + \text{TP} + \text{FN} + \text{FP}) \quad (21)$$

All possible combinations of TPR and FPR compose a receiver operating characteristic (ROC) space. The area under the ROC curve, or simply AUC, provides a good "summary" for the accuracy of the classifier. Table I gives the value of these performance indices. This demonstrates a high success rate of classifier in classifying the events. The contour plot for remaining classifier is not shown due to space restriction.

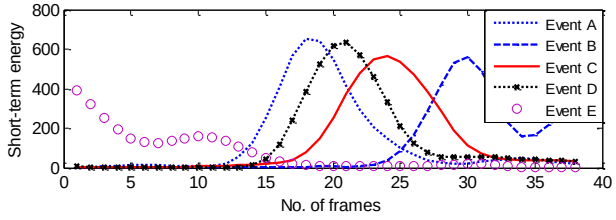

(a) Short term energy for event segments

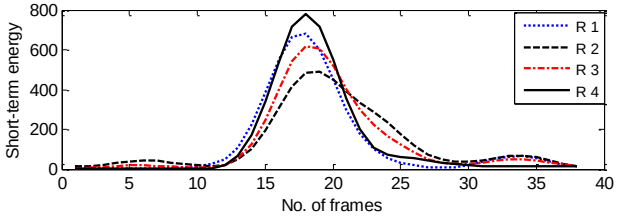

(b) Short term energy for event- A

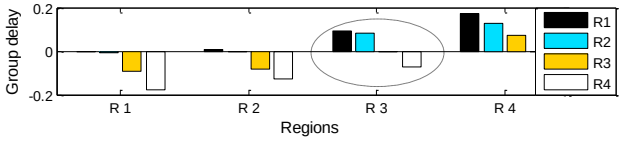

(c) Group delay of Event A

Figure 8. Event signal characterization

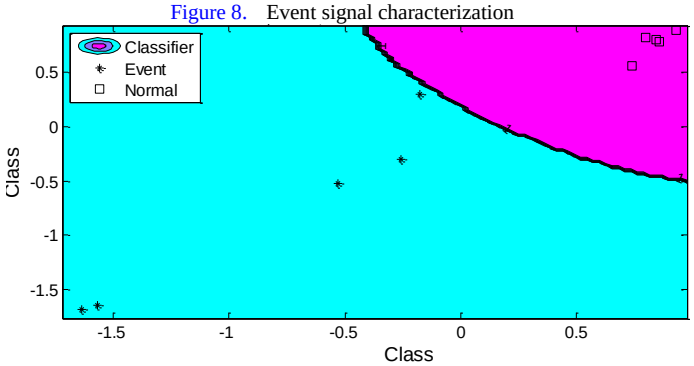

(a) Between signals of event A and post-event (Normal) condition

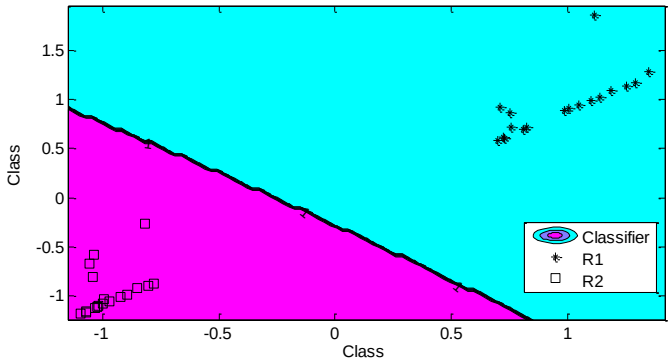

(b) Between signals of all events from regions R1 & R2
Figure 9. Classification of signal characterisic for event

TABLE I CLASSIFIER PERFORMANCE INDICES

Classifier	Events between	Indices			
		TPR	FPR	DA	AUC
Binary class	Event vs post-event (Normal)	0.7589	0.2562	98.00	0.9845
Binary class	R1 vs R2	0.7639	0.2639	100.00	1.0
Multi-class	R1 vs R2 vs R3 vs R4	0.7724	0.2542	100	0.9988
Binary class	R1 & R3 vs R2 & R4	0.7563	0.2580	94.29	0.9984

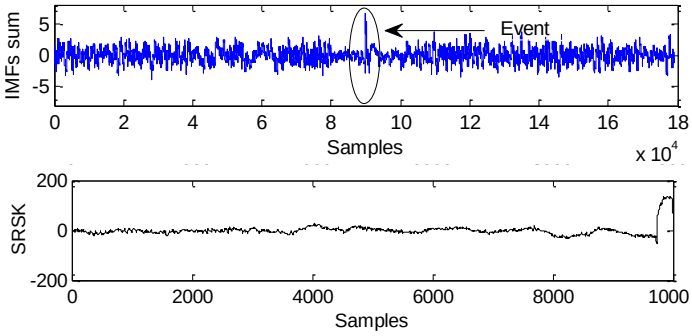

(a) Sum of IMF of voltage magnitude and its SRSK on 9th segment

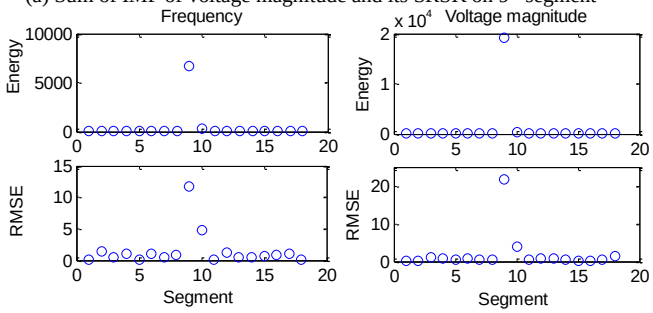

(b) Computed indices on voltage magnitude and frequency
Figure 10. Analysis using EMD for signals of case I

B. Nordic Grid Data

If any event occurrence involving fault is sufficiently long, subsequently, the post-fault dynamics may result in larger deviations from the steady state and significant uncertainty in the resulting dynamical trajectory [28]. This motivates the need for analysis on post-event dynamics to ascertain the convergence to steady state. Thus, the proposed approach is applied on complete length of data stream. The sum of IMFs computed from each data segment (10000 samples) is shown in Fig. 10. The transient suggesting an event is indicated very well in the 9th segment in Fig.10(a) (upper subplot). The variation of sum of IMF and computation of SRSK for 9th segment is shown in lower subplot of said figure. The sum of IMF indicates abrupt change which means spectral activity caused by event occurrence in the 9th segment. The trailing end of event samples belongs to the 10th segment. The maximum energy and RMSE calculated for complete data segment is shown in Fig.10(b). This confirms that the proposed scheme successfully detects the event in 9th segment. The event is however not captured in the 10th segment. The segment containing no event information is not associated with any transient and thus their indices values remain comparatively low. It can be seen that energy and RMSE computed on SRSK-IMF of V (voltage) signal in relation to F_r

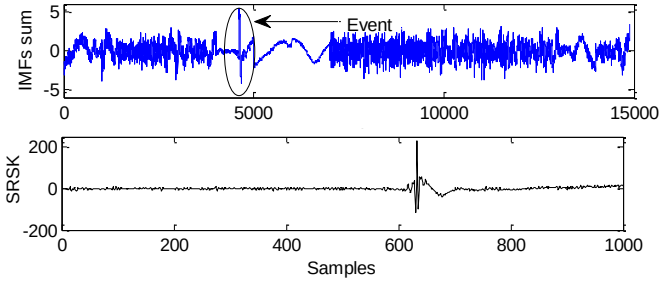

(a) Sum of IMF of frequency and its SRSK on 5th segment

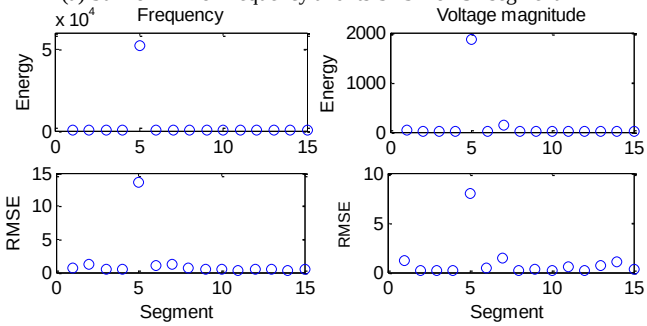

(b) Computed indices on voltage magnitude and frequency
Figure 11. Analysis using EMD for signals of case II

(frequency) signal is higher and thus correlates to indicate the reactive power change/disturbance type of event. The scalability of detection scheme is tested in terms of varied size of samples in the segment depending upon the measurements length. Similarly, in another study (case II) of Nordic grid PMU data, the above analysis is performed on frequency signal and results are shown in Fig. 11. The 5th segment is found to contain event information. The detection scheme highlights the specific changes in the PMU measurements as a result of captured transients on the network. The segment length consists of 1000 samples. The maximum energy and RMSE indices yield transient disturbance on 5th segment, thus clearly distinct the rest of segment of time series data as shown in Fig.11(b). The segment associated with transient is very well recognized. Under normal conditions, these indices remain low in amplitude. Unlike above discussion (Case I), the computed indices from SRSK-IMF of F_r signal is observed to be higher than V signal and thus, the event is related to active power change/disturbance type. This may be interpreted as a sudden drop of active power caused due to transmission line trip. The above discussion also suggests that the size of

sample in the data segment does not influence the performance of proposed detection scheme.

VI. Conclusions

The implementation of event detection, its characterization and classification using signal processing techniques was proposed in the paper. The event detection step does not involve computation of threshold in normal conditions. The computation of SRSK on IMF sum is more suitable for event detection than those based on WC. Several case studies on PMU data had shown that the proposed approach can facilitate in detecting and discriminate events which could serve as input information to an automatic recognition system. The intuition behind the analysis of so many PMU signals was to suggest relevant signal indicating a particular type of event.

It was shown that signals from different regions, though interconnected to each other reveal distinct characteristic following the event occurrence in NASPI PMU signals. For instance, SVM was capable to distinguish the event signals of region R1 against those of region R2. For physical disturbance involving active power mismatch associated with high amplitude oscillations having good damping, frequency signal is most effective event indicator, otherwise it is angle signal. Following the active power unbalance disturbance, the angle oscillations die out according to damping effect in each region.

The study had considered using not only angle and frequency, but also voltage magnitude for event detection. In the analysis of PMU data from Nordic grid, it was apparent that the signal associated with particular type of event provided information on the disturbance type. The analysis on event associated signal signifies the type of physical disturbance, i.e. whether active power or reactive power change.

Unlike recently reported event detection scheme, the proposed approach on event detection and its signal characterization was successfully demonstrated on different number of samples in the segment. It could therefore be useful for providing visual alerts, allowing to detect events in real-time.

Acknowledgement

The authors acknowledge the receipt of research support on project “Operation of the Smart Grid with Wide Area Information (OperaGrid)” by DST-RCN of the two countries (Indo-Norway Joint Proposal).

References

[1] J. De La Ree, V. Centeno, J. S. Thorp and A. G. Phadke, Synchronized phasor measurement applications in power systems, *IEEE Trans. on Smart Grid*, vol. 1, no. 1, pp. 20-27, June 2010.

[2] Math H.J. Bollen, Irene Y.H. Gu,Surya Santoso, Mark F. McGranaghan, Peter A. Crossley, Moisés V. Ribeiro, and Paulo F. Ribeiro, Bridging the gap between signal and power, *IEEE Sig. Proc. Mag.*, pp. 12-31, July 2009.

[3] D. Novosel, V. Madani, B. Bhargava, K. Vu, J. Cole, Dawn of the grid synchronization, *IEEE Power and Energy Magazine*, Vol. 6, no. 1,pp. 49-60, 2008.

[4] P. M. Ashton, G. A. Taylor, A. Carter, and W. Hung, Application of phasor measurement units to estimate power system inertial frequency response, in *Proc. IEEE Power Eng. Soc. Gen. Meeting*, Vancouver, BC, Canada, Jul. 2013, pp. 1–5.

[5] J. E. Tate, Event detection and visualization based on phasor measurement units for improved situational awareness, Ph.D. dissertation, Dept. Elect. Comput. Eng., Univ. Illinois, Urbana-Champaign, IL, USA, 2008.

[6] K. Mei, S. M. Rovnyak, C. Ong, Design aspect for wide-area monitoring and control system, *IEEE Trans. Power Syst.*, vol. 23, no. 2, pp. 673–679, May 2008.

[7] A. J. Allen, S. Sohn, S. Santoso, W. M. Grady, Algorithm for screening PMU data for power system events, in *Proc. IEEE Int. Conf. Innov. Smart Grid Technol.*, Berlin, Germany, Oct. 2012, pp. 1–6.

[8] B. McCamish et al., A data driven framework for real-time power system event detection and visualization, arXiv:1501.04038.

[9] Ti Xu, T. Overbye, Real-time event detection and feature extraction using PMU measurement data, in *Proc. IEEE Int. Conf. on Smart Grid Comm. (SmartGridComm): Data Mgt, Grid Ana. and Dynamic Pricing*, Miami, USA. 2015, pp. 265-270.

[10] M. Khan, P. M. Ashton, M. Li, G. A. Taylor, I. Pisica, J. Liu, Parallel detrended fluctuation analysis for fast event detection on massive PMU data, *IEEE Trans. on Smart Grid*, vol. 6, pp. 360-368, 2015.

[11] S.A. Lavand, G.R. Gajjar, S.A. Soman, R. Gajbhiye, Mining spatial frequency time series data for event detection in power systems, in *Proc. 13th Int. Conf. on Develop. in Power Syst. Prot.* (DPSP), 7-10 March 2016, Edinburgh, UK.

[12] I. Y. H. Gu, M.H. J. Bollen and E. Styvaktakis, The use of time-varying AR model for the characterization of voltage disturbances, in *Proc. IEEE Power Engineering Society Winter Meeting*, vol. 4, pp. 2943-2948, 2000.

[13] G. Wang, J. Jiao, S. Yin, A kernel direct decomposition based monitoring approach for nonlinear quality-related fault detection, *IEEE Trans. on Industrial Informatics*, Online published, 2017.

[14] Y. Zhou et al. Abnormal event detection with high resolution micro-PMU data, *in Proc. 2016 Power Syst. Comp. Conf. (PSCC)*, Genoa, Italy, June 20-24, 2016.

[15] S. Santoso, W. M. Grady, E. J. Powers, J. Lamoree, S. C. Bhatt, Characterization of distribution power quality events with Fourier and wavelet transforms, *IEEE Trans. Power Delivery*, vol. 15, no. 1, pp.247-254, Jan. 2000.

[16] S-W Sohn, A.J. Allen, S. Kulkarni, W. M. Grady,S. Santoso, Event detection method for the PMUs synchrophasor data, in *Proc. of IEEE Power Electronics and Machines in Wind Applications*, pp.1-7,16-18 July 2012, Denver, CO, 2012.

[17] F. B. Costa, Fault-induced transient detection based on real-time analysis of the wavelet coefficient energy, *IEEE Trans. Power Del*., vol. 29, no. 1, pp. 140–153, Feb. 2014.

[18] D-I. Kim, T. Y. Chun, S. H. Yoon, G. Lee, and Y.-J. Shin, Wavelet-Based Event Detection Method Using PMU Data, *IEEE Trans. on Smart grid*, vol. 8, pp. 1154-1162, 2017.

[19] M. Biswal, S. M. Brahma,H. Cao, Supervisory protection and automated event diagnosis using PMU data, *IEEE Trans. on Power Del*., vol. 31, pp. 1855-1863, 2016.

[20] N. E. Huang, et al. The empirical mode decomposition and the Hilbert spectrum for nonlinear and non-stationary time series analysis. *Proc. of the Royal Society of London*, Series A, 454, pp. 903-995, 1998.

[21] P. Flandrin, G. Rilling, and P. Goncalves, Empirical mode decomposition as a filter bank, *IEEE Signal Proc.* Let., Vol. 11, no. 2, pp.112–114, 2004.

[22] R.F. Dwyer, Detection of non-Gaussian signals by frequency domain kurtosis estimation in *Proc International Conference on Acoustic, Speech and Signal Processing*, Boston, 1983, pp. 607–610.

[23] J.Zhu, Z. Ge, Z. Song, Distributed parallel PCA for modeling and monitoring of large-scale plant-wide processes with big data, *IEEE Trans. on Ind. Infor*., Online published, 2017.

[24] T. Barszcz, R. B. Randall, Application of spectral kurtosis for detection of a tooth crack in the planetary gear of a wind turbine, *Mech. Sys. and Sig. Proc*., Vol. 23, pp.1352–1365, 2009.

[25] L. Saidi, J. B. Ali, F. Fnaiech, The use of spectral kurtosis as a trend parameter for bearing faults diagnosis, in *Proc. of 15th international conference on Sciences and Techniques of Automatic control & Computer Engineering* - STA'2014, Hammamet, Tunisia, December 21-23, 2014.

[26] J. Antoni, The spectral kurtosis: a useful tool for characterising non-stationary signals, *Mech. Sys. and Sig. Proc*., Vol. 20, pp. 282–307, 2006.

[27] Ming Zhao, Jing Lin, Xiaoqiang Xu, Xuejun Li, Multi-Fault detection of rolling element bearings under harsh working condition using IMF-based adaptive envelope order analysis, *Sensors* 2014, *14*, 20320-20346.
[28] P. M. Ashton *et al.*, Novel application of detrended fluctuation analysis for state estimation using synchrophasor measurements, *IEEE Trans. Power Syst.*, vol. 28, no. 2, pp. 1930–1938, 2013.
[29] T. Thiruvaran, E. Ambikairajah, M. Epps, Group delay features for speaker recognition, in *Proc. Int. Conf Information, Comm. Signal Process*., 2007, pp. 1–5.
[30] P. K. Ray, N. Kishor, S. R. Mohanty, Islanding and power quality disturbance detection in grid-connected hybrid power system using wavelet and S-transform, *IEEE Trans. on Smart Grid*, vol. 3, no. 3, pp. 1082-1094, 2012.
[31] https://www.naspi.org
[32] http://www.lexjansen.com/nesug/nesug10/hl/hl07.pdf

Authors

Sanjay Singh Negi received B.Tech from REC (now NIT), Hamirpur in Electrical Engineering in 1991 and completed M.Tech from REC (now NIT) Kurukshetra in Power System in 1993. Since November 1993, he is working wih Indian Railways. Presently, Mr. Negi is posted at North Central Railway Head Quarters office Allahabad as Dy. General Manager. He has interest in the area of wide area monitoring of power system for fault diagnosis, event analysis, etc.
Email: kinnaursanjay@yahoo.co.in

Nand Kishor (SM'12) received the Ph.D. degree from Indian Institute of Technology (IIT), Roorkee, India. Presently, he is working as Associate Professor in Electrical Engineering Department, MNNIT Allahabad, India. His research area includes AI applications in power system, Wireless sensor systems, Distributed generation with renewable resources, WAMS, Smart grid technologies**.**
Email: nand_research@yahoo.co.in

Kjetil Uhlen (M'95) received the M.Sc. degree and the Ph.D. degree in control engineering from the Norwegian Institute of Science and Technology (NTNU), Trondheim, Norway, in 1986 and 1994, respectively. Kjetil Uhlen is professor in Power Systems at the Norwegian University of Science and Technology (NTNU), Trondheim, and a Special Adviser at STATNETT (the Norwegian TSO). His main areas of work include research and education in control and operation of power systems, power system dynamics and wind power integration.
Email: kjetil.uhlen@ntnu.no

Richa Negi completed B.Tech in Electrical Engineering and M.Tech (power System) from REC (now NIT) Kurukshetra in 1992 and 1994 respectively. She received Ph.D in the area of control System from MNNIT, Allahabad in 2013. Presently, she is working as Associate Profesor in the Department of Electrical Engineering, MNNIT Allabhabad. Her area of research interest includes multi-diamensional control system, non-linear control and systems, WAMS and smart grid.
Email: richa@mnnit.ac.in